Enzyme Catalysis and Regulation:

X-ray Crystallographic Analysis of the 6-Aminohexanoate Cyclic Dimer Hydrolase: CATALYTIC MECHANISM AND EVOLUTION OF AN ENZYME RESPONSIBLE FOR NYLON-6 BYPRODUCT DEGRADATION

Kengo Yasuhira, Naoki Shibata, Go Mongami, Yuki Uedo, Yu Atsumi, Yasuyuki Kawashima, Atsushi Hibino, Yusuke Tanaka, Young-Ho Lee, Dai-ichiro Kato, Masahiro Takeo, Yoshiki Higuchi and Seiji Negoro

J. Biol. Chem. 2010, 285:1239-1248.
doi: 10.1074/jbc.M109.041285 originally published online November 3, 2009

THE JOURNAL OF BIOLOGICAL CHEMISTRY VOL. 285, NO. 2, pp. 1239–1248, January 8, 2010

X-ray Crystallographic Analysis of the 6-Aminohexanoate Cyclic Dimer Hydrolase

CATALYTIC MECHANISM AND EVOLUTION OF AN ENZYME RESPONSIBLE FOR NYLON-6 BYPRODUCT DEGRADATION[*] [S]

Received for publication, July 13, 2009, and in revised form, October 14, 2009 Published, JBC Papers in Press, November 3, 2009, DOI 10.1074/jbc.M109.041285

Kengo Yasuhira[‡1], Naoki Shibata[§¶1], Go Mongami[‡], Yuki Uedo[‡], Yu Atsumi[‡], Yasuyuki Kawashima[‡], Atsushi Hibino[‡], Yusuke Tanaka[‡], Young-Ho Lee[‖], Dai-ichiro Kato[‡], Masahiro Takeo[‡], Yoshiki Higuchi[§¶2], and Seiji Negoro[‡3]

From the [‡]Department of Materials Science and Chemistry, Graduate School of Engineering, University of Hyogo, Hyogo 671-2201, the [§]Department of Life Science, Graduate School of Life Science, University of Hyogo, Hyogo 678-1297, the [¶]RIKEN Harima Institute, SPring-8 Center, Hyogo 679-5148, and the [‖]Institute for Protein Research, Osaka University, Osaka 565-0871, Japan

We performed x-ray crystallographic analyses of the 6-aminohexanoate cyclic dimer (Acd) hydrolase (NylA) from *Arthrobacter* sp., an enzyme responsible for the degradation of the nylon-6 industry byproduct. The fold adopted by the 472-amino acid polypeptide generated a compact mixed α/β fold, typically found in the amidase signature superfamily; this fold was especially similar to the fold of glutamyl-tRNA^{Gln} amidotransferase subunit A (z score, 49.4) and malonamidase E2 (z score, 44.8). Irrespective of the high degree of structural similarity to the typical amidase signature superfamily enzymes, the specific activity of NylA for glutamine, malonamide, and indoleacetamide was found to be lower than 0.5% of that for Acd. However, NylA possessed carboxylesterase activity nearly equivalent to the Acd hydrolytic activity. Structural analysis of the inactive complex between the activity-deficient S174A mutant of NylA and Acd, performed at 1.8 Å resolution, suggested the following enzyme/substrate interactions: a Ser^{174}-*cis*-Ser^{150}-Lys^{72} triad constitutes the catalytic center; the backbone N in Ala^{171} and Ala^{172} are involved in oxyanion stabilization; Cys^{316}-S$^{\gamma}$ forms a hydrogen bond with nitrogen (Acd-N^{7}) at the uncleaved amide bond in two equivalent amide bonds of Acd. A single S174A, S150A, or K72A substitution in NylA by site-directed mutagenesis decreased the Acd hydrolytic and esterolytic activities to undetectable levels, indicating that Ser^{174}-*cis*-Ser^{150}-Lys^{72} is essential for catalysis. In contrast, substitutions at position 316 specifically affected Acd hydrolytic activity, suggesting that Cys^{316} is responsible for Acd binding. On the basis of the structure and functional analysis, we discussed the catalytic mechanisms and evolution of NylA in comparison with other Ser-reactive hydrolases.

Nylon-6 is produced by ring cleavage polymerization of ϵ-caprolactam and consists of more than 100 units of 6-aminohexanoate. During the polymerization reaction, however, some molecules fail to polymerize and remain oligomers, whereas others undergo head-to-tail condensation to form cyclic oligomers (1, 2). These byproducts (designated nylon oligomers) contribute to an increase in industrial waste material into the environment. Therefore, biodegradation of the xenobiotic compounds is important in terms of environmental points of view. In addition, the biological system for degradation provides us with a suitable system to study how microorganisms have evolved specific enzymes responsible for this degradation (1, 2).

Previous biochemical studies in a nylon oligomer-degrading bacterium *Arthrobacter* sp. strain KI72 have revealed that three enzymes, 6-aminohexanoate cyclic dimer hydrolase (NylA),[4] 6-aminohexanoate dimer hydrolase (NylB), and endo-type 6-aminohexanoate oligomer hydrolase (NylC), are responsible for the degradation of nylon oligomers (1, 2). NylA specifically hydrolyzes one of the two equivalent amide bonds in Acd, generating a 6-aminohexanoate linear dimer (Ald) (see Fig. 1*A*). However, NylA is barely active on Ald (substrate for NylB), 6-aminohexanoate cyclic oligomers (degree of polymerization > 3, substrates for NylC), and more than 60 kinds of various amide compounds, including peptides and β-lactams (1–3). NylA is a homodimeric enzyme, and Acd hydrolytic activity is inhibited by diisopropylfluorophosphate, a Ser-enzyme-specific inhibitor, suggesting that Ser is involved in the catalytic function (3). NylA has also been found in *Pseudomonas* sp. NK87 and six alkalophilic strains, including *Kocuria* sp. KY2 (4–6). All of the NylA proteins identified so far have been

* This work was supported in part by a grant-in-aid for scientific research from the Japan Society for Promotion of Science and by grants from the Global Centers of Excellence Program, the National Project on Protein Structural and Functional Analyses, the Core Research for Evolutional Science and Technology Program, "Development of the Foundation for Nano-Interface Technology" from JST, and the Japan Aerospace Exploration Agency project.

[S] The on-line version of this article (available at http://www.jbc.org) contains supplemental Table S1 and Figs. S1–S4.

The atomic coordinates and structure factors (codes 3A2P and 3A2Q) have been deposited in the Protein Data Bank, Research Collaboratory for Structural Bioinformatics, Rutgers University, New Brunswick, NJ (http://www.rcsb.org/).

[1] These authors contributed equally to this work.

[2] To whom correspondence may be addressed: Dept. of Life Science, Graduate School of Life Science, University of Hyogo, 3-2-1 Koto, Kamigori-cho, Ako-gun, Hyogo 678-1297, Japan. Tel. and Fax: 81-791-58-0179; E-mail: hig@sci.u-hyogo.ac.jp.

[3] To whom correspondence may be addressed: Dept. of Materials Science and Chemistry, Graduate School of Engineering, University of Hyogo, 2167 Shosha, Himeji, Hyogo 671-2280, Japan. Tel. and Fax: 81-792-67-4891; E-mail: negoro@eng.u-hyogo.ac.jp.

[4] The abbreviations used are: NylA, 6-aminohexanoate cyclic dimer hydrolase; Acd, 6-aminohexanoate cyclic dimer; Ald, 6-aminohexanoate linear dimer; NylA-A^{174}, NylA containing the S174A substitution; AS, amidase signature; GatA, glutamyl-tRNA^{Gln} amidotransferase subunit A; MAE2, malonamidase E2; PAM, peptide amidase.

found to be immunologically identical and possess similar subunit molecular masses of 52 kDa (5, 6). NylA from *Pseudomonas* is 99% identical in amino acid sequence to the homolog from *Arthrobacter*, and both *nylA* genes are encoded on a plasmid (4, 7).

NylA is classified as an amidase signature (AS) superfamily protein, characterized by the presence of a conserved stretch of ~130 amino acid residues (AS sequence) (8–21). AS superfamily enzymes are widely distributed among microorganisms, animals, and plants; they are involved in various biological functions, including transamidation of misacylated Glu-tRNA^{Gln} (8, 9), formation of the plant hormone indoleacetic acid (10, 11), and hydrolysis of malonamide (12, 13), fatty acid amides (14, 15), and peptide amides (16, 17). In addition, amidases from *Rhodococcus rhodochrous* and *Sulfolobus solfataricus* possess nitrilase activity, catalyzing the cleavage of the carbon-nitrogen triple bond in a nitrile (18, 19). Recently, NylA from *Arthrobacter* was also shown to exhibit 98% homology to ω-laurolactam hydrolase from *Rhodococcus* (dbj|BAG70960.1|), *Cupriavidus* (dbj|BAH09869.1|), and *Sphingomonas* (dbj|BAH09872.1|), which are potentially used for production of 12-aminolauryl acid (material for nyon-12 production) (20). Moreover, NylA is closely related to an aryl acylamidase from *Nocardia farcinica*, which cleaves the amide bond in a polyamide model compound (adipic acid *bis*hexylamide) and the ester bond in *bis*(benzoyloxyethyl)terephthalate and increases the hydrophilicity of polyamide 6 (21). Thus, from fundamental, industrial, and environmental points of view, it would be interesting to know the structural factors that determine the unique substrate specificity of NylA recognizing a cyclic amide compound having 6-aminohexanoate as a monomeric unit.

Recently, we have reported the crystallization conditions of NylA from strain KI72 (22). In this paper, we performed x-ray crystallographic analysis of NylA, identified the amino acid residues responsible for catalytic function based on the three-dimensional structures, estimated the catalytic mechanisms, and discussed the evolution of nylon oligomer-degrading enzymes.

EXPERIMENTAL PROCEDURES

Plasmids and Site-directed Mutagenesis

The hybrid plasmid pUEFA, containing a wild-type *nylA* gene in the vector pUC18, was used as the parental plasmid DNA (22). To obtain mutant enzyme versions of NylA, site-directed mutagenesis was carried out by the modification of restriction site method (23) (for K72A, S150A, S174A, C316G, C316D, C316E, and C316S substitutions) or PrimeSTAR mutagenesis kit (Takara Bio Inc., Otsu, Japan) (for N125A, C316A, C316K, and C316N substitutions) using the primers shown in supplemental Table S1 and plasmid pUEFA as a template DNA. After sequencing the entire *nylA* region, we confirmed that a single desired substitution was integrated in the wild-type *nylA* sequence, and recombinant plasmid expressing the mutant *nylA* genes were constructed using the pUC18 vector, as described previously (22).

Enzyme Purification

Because cultivation at temperatures 30 °C or higher results in insoluble NylA, *Escherichia coli* JM109 cells expressing NylA and mutant enzymes were grown at 25 °C, as described previously (22). Buffer A (20 mM phosphate buffer containing 10% glycerol, pH7.0) was used throughout for purification. Cell extracts obtained by ultrasonication were used as crude enzyme. NylA and its mutant enzymes were fractionated by $(NH_4)_2SO_4$ (25–55% saturated). The enzyme sample dissolved in buffer A was desalted using a PD-10 desalting column (GE Healthcare), and the protein-containing fractions were loaded onto a Hi-Trap Q-Sepharose (GE Healthcare) column equilibrated with buffer A. After the column was washed with buffer A, the enzyme was eluted by increasing the NaCl concentration from 0 to 0.25 M (22). Fractions containing NylA or its mutants were identified as highly expressed 52-kDa bands on SDS-PAGE, which were absent in cell extracts of *E. coli* JM109 harboring pUC18. At the final stage, the enzymes were judged to be homogeneous by analyzing the SDS-PAGE, native PAGE, and light-scattering diffraction patterns.

Assay

To measure Acd hydrolase activity, enzyme reactions were performed at 30 °C using 10 mM Acd (in buffer A) (standard assay condition). Amino groups liberated by the reaction were quantified by colorimetry using trinitrobenzenesulfonic acid (3). Enzyme reactions were similarly performed using 20 mM malonamide (malonamidase activity) or 20 mM indoleacetamide (indoleacetamide hydrolase activity), and release of ammonia formed by the hydrolytic reactions was quantified by colorimetry using trinitrobenzenesulfonic acid (3).

For kinetic study, Acd hydrolytic activity was assayed under standard assay conditions, except that various concentrations of Acd were used. Kinetic parameters (k_{cat} and K_m values) were evaluated by directly fitting the Michaelis-Menten equation to the data using GraphPad prism, version 5.01 (GraphPad, San Diego, CA). The k_{cat} values were expressed as turnover numbers/subunit (M_r of the subunit: 53,000).

For semi-quantitative detection of Acd hydrolase and glutaminase activity, the enzyme reactions were performed using purified NylA (0.1–1 mg/ml) and 10 mM Acd or 20 mM Gln. After the reaction proceeded at 30 °C for 2–48 h, 10-μl aliquots were sampled, and the reactions were stopped by incubating the aliquots in boiling water for 3 min. The reaction mixtures (1 μl) were spotted onto a silica gel plate. The samples were developed by solvent mixture (1-propanol:water:ethyl acetate:ammonia = 24:12:4:1.3), and degradation products were detected by spraying with 0.2% ninhydrin solution (in butanol saturated with water) (6).

To measure carboxylesterase activity, enzyme reactions were performed at 30 °C using 0.2 mM each of *p*-nitrophenylacetate (C2-ester), *p*-nitrophenylbutyrate (C4-ester), and *p*-nitrophenyloctanoate (C8-ester) dissolved in 50 mM phosphate buffer containing 0.43% Tween 20 (pH 7.0). The release of *p*-nitrophenol ($\epsilon_{400\,nm}$ = 6,710 M^{-1} cm^{-1}) was assayed by absorbance at 400 nm. As a control, we confirmed that spontaneous hydrolysis of *p*-nitrophenylesters in buffer A is not observed during the 30 min of the reaction. Carboxylesterase activities were assayed in triplicate, and the average values and standard errors were calculated.

Crystallographic Analysis

Crystallization and Data Collection of Diffraction—Hexagonal prismatic crystals (0.3 × 0.3 × 0.5 mm) were obtained by the

sitting drop vapor diffusion method as reported previously (22). The droplets were prepared by mixing 2–3 μl of purified NylA solution (10 mg ml^{-1} protein in 20 mM phosphate buffer containing 10% glycerol, pH 7.3) and the same volume of reservoir solution containing 1.0 M sodium citrate as a precipitant in 0.1 M imidazole buffer (pH 8.0) and 12.5% glycerol and equilibrated against 100 μl of reservoir solution at 10 °C. The crystal belonged to space group $P6_2$, with unit cell parameters $a = b = 130.75$, $c = 58.23$ Å (see Table 1). For native crystals, the crystals were soaked for 24 h in cryoprotectant solution (1.0 M sodium citrate, 0.1 M imidazole, pH 8.0, 25% glycerol). Heavy atom derivatives were prepared by soaking the crystals for 24 h in cryoprotectant solution containing 1 mM $HgCl_2$. For analysis of enzyme·substrate complexes, the activity-deficient S174A mutant of NylA (NylA-A^{174}) was used to prevent hydrolysis of the substrate during crystallographic analysis. the NylA-A^{174}·Acd complex was prepared by soaking the crystals in the cryoprotectant solution containing 20 mM Acd for 3 h. Cryocooling was performed by blowing cold nitrogen steam onto the crystals at 100 K. The diffraction data sets of the NylA crystal and NylA-A^{174}·Acd complex were collected at the SPring-8 (Hyogo, Japan) Beamlines BL38B1 (equipped with a Rigaku Jupiter CCD detector system) and BL41XU (equipped with an ADSC Quantum 315 detector system), respectively. For $HgCl_2$ derivatives, diffraction data were recorded on Beamline BL-5A at the Photon Factory (Tsukuba, Japan) using an ADSC Quantum 315 detector system. The following parameters were chosen for data collection: wavelength, 1.0000 Å; crystal to detector distance, 180 mm for native crystals, 300 mm for mercury derivatives, and 200 mm for NylA-A^{174}·Acd complexes; oscillation range/image, 0.5° for native crystals and mercury derivatives or 1.0° for NylA-A^{174}·Acd complexes. Indexing, integration, and scaling of reflections were performed using the HKL2000 program package (24). The diffraction data were collected from native NylA crystal, NylA-mercury (II) dichloride derivative, and NylA-A^{174}·Acd complex crystal to resolutions of 1.90, 2.06, and 1.80 Å, respectively (see Table 1).

Phase Determination, Model Building, and Crystallographic Refinement—The NylA structure was determined by the single wavelength anomalous diffraction method using the $HgCl_2$ derivative data. The mercury substructure for the derivative crystal was solved at 2.1 Å resolution by the program BnP (25) using the anomalous signal of the mercury atoms. Initial phase parameters were determined using the program SHARP (26). The electron density map was automatically traced with ARP/wARP. The models for the untraced regions, except for amino acids at position 1–4, 19–26, 403–410, and 486–493, were constructed by manual model building using XFIT (27). Rigid body refinement was performed using the coordinates of the initial model to fit the unit cell of the NylA crystal, followed by positional and B-factor refinement with the program CNS (28). For the NylA-A^{174}·Acd complex, rigid body refinement was performed using the coordinates of the refined NylA structure to fit the unit cell of the NylA-A^{174}·Acd complex, followed by positional and B-factor refinement with the program CNS. With several cycles of a manual model rebuilding by XFIT, R-factor and R_{free} were 18.1 and 19.5% (for NylA) and 18.3 and 19.5% (for the NylA-A^{174}·Acd complex), respectively. The Molprobity (29) Ramachandran analysis showed 467 residues (97.1%) in favored regions, 481 residues (99.8%) in allowed regions, and 1 residue (Thr^{75}) (0.2%) in outliers for NylA and 465 residues (96.9%) in favored regions, 479 residues (99.8%) in allowed regions, and 1 residue (Ser^{416}) (0.2%) in outliers for the NylA-A^{174}·Acd complex. The electron density map of Thr^{75} and Ser^{416}, located in outliers, was clear enough to assign the structures without ambiguity. The results of the crystal structure analysis are summarized in Table 1. Figures of three-dimensional models of proteins were generated with the program MolFeat (version 3.6; FiatLux Co., Tokyo, Japan).

RESULTS AND DISCUSSION

Overall Structure of NylA and Structural Comparison with Proteins in Protein Data Bank

The structure of NylA from *Arthrobacter* sp. KI72 was solved with single anonymous dispersion phasing using a mercury derivative crystal of the enzyme at 2.2 Å resolution, and models of the native enzymes were constructed at 1.9 Å resolution (Table 1). NylA consists of a single polypeptide chain of 472 amino acid residues (3). The overall structure of the molecule is a compact mixed α/β fold containing a central irregular β-sheet composed of 11 β-strands surrounded by 20 α-helices. Each β-strand is sequentially rotated in the same direction with respect to an adjacent β-strand, such that the β-strand at one end of the molecule is rotated ~180° relative to the β-strand at the other end of the molecule (see Fig. 2*A*). A homology search based on the NylA structure was carried out using the DALI program. Among the ~55,000 proteins registered in the Protein Data Bank, five proteins classified as "AS superfamily," glutamyl-$tRNA^{Gln}$ amidotransferase subunit A (GatA) (z score, 49.4) (Protein Data Bank code 2df4) (9), probable amidase (z score, 45.0) (Protein Data Bank code 2dc0), malonamidase E2 (MAE2) (z score, 44.8) (Protein Data Bank code 1ocm) (12), peptide amidase (PAM) (z score, 44.0) (Protein Data Bank code 1m21) (16), and fatty acid amide hydrolase (z score, 38.2) (Protein Data Bank code 1mt5) (14), and their mutants were extracted as proteins with high z scores. The z scores of other proteins in Protein Data Bank were found to be lower than 4.5.

Bacterial glutamyl-$tRNA^{Gln}$ amidotransferase is a heterotrimer (GatCAB). GatA receives top scores in a Protein Data Bank homology search; the protein possesses glutaminase activity for generating an ammonia donor for recruitment of the amidotransferase reaction of misacylated Glu-$tRNA^{Gln}$ to a corrected Gln-$tRNA^{Gln}$. MAE2 and PAM catalyze the hydrolysis of malonamide and peptide amide, respectively. Fatty acid amide hydrolase is a transmembrane protein that catalyzes the hydrolysis of fatty-acid amide. Functionally, GatA, MAE2, and PAM catalyze the hydrolysis of terminal amide bonds, releasing ammonia, whereas NylA specifically hydrolyzes internal amide linkages of Acd (Fig. 1). Although "probable amidase" (Protein Data Bank code 2dc0) was extracted as the second highest z score, its function has not been identified. Accordingly, structural and functional comparison mainly focuses on GatA, MAE2, and PAM, which have z scores higher than 40.

The structurally superimposable regions comprise 451 residues (GatA), 405 residues (MAE2), or 439 residues (PAM), and

TABLE 1

Data collection statistics

The values in parentheses are for the outer resolution shell.

Data collection	NylA (native)	NylA-A^{174}·Acd complex	Mercury (II) chloride derivative
Space group	$P6_2$	$P6_2$	$P6_2$
Unit cell $a = b$ (Å)	130.75	130.66	131.39
c (Å)	58.23	58.63	58.07
Wavelength (Å)	1.0000	1.0000	1.0000
Resolution (Å)	30-1.90 (1.97-1.90)	30-1.80 (1.86-1.80)	30-2.06 (2.13-2.06)
Total reflections	485,579	567,837	363,039
Unique reflections	44,300 (4,021)	52,953 (5,212)	34,955 (2,980)
Completeness (%)	98.6 (90.4)	99.7 (99.1)	97.2 (82.3)
R_{merge} (%)	3.8 (30.4)	5.4 (48.9)	5.8 (33.4)
$<I>/<\sigma(I)>$	24.5 (5.2)	22.3 (5.0)	16.5 (6.6)
Phasing			
Figure of merit, centric/acentric			0.106/0.380
Phasing power			1.67
R_{Curris}			0.649
Refinement			
Resolution range (Å)	28.0–1.90 (1.97–1.90)	50–1.80 (1.86–1.80)	
R_{work} (%)[a]	18.1 (26.2)	18.7 (27.9)	
R_{free} (%)[b]	21.4 (28.4)	22.2 (33.0)	
No. of protein atoms	3,602	3,592	
No. of ligand atoms	0	16	
No. of water molecules	445	521	
Root mean square bond distances (Å)	0.005	0.005	
Root mean square bond angles (°)	1.2	1.2	
Average B-factor			
Protein	38.6	35.0	
Ligand		45.7	
Solvent	50.3	47.9	

[a] $|R_{work} = \Sigma_{hkl}||F_{obs}| - k|F_{calc}||(\Sigma_{hkl}|F_{obs}|)^{-1}$; k, scaling factor.
[b] $R_{work} = \Sigma_{hkl}||F_{obs}| - k|F_{calc}||(\Sigma_{hkl}|F_{obs}|)^{-1}$, where all of the reflections belong to a test set of randomly selected data.

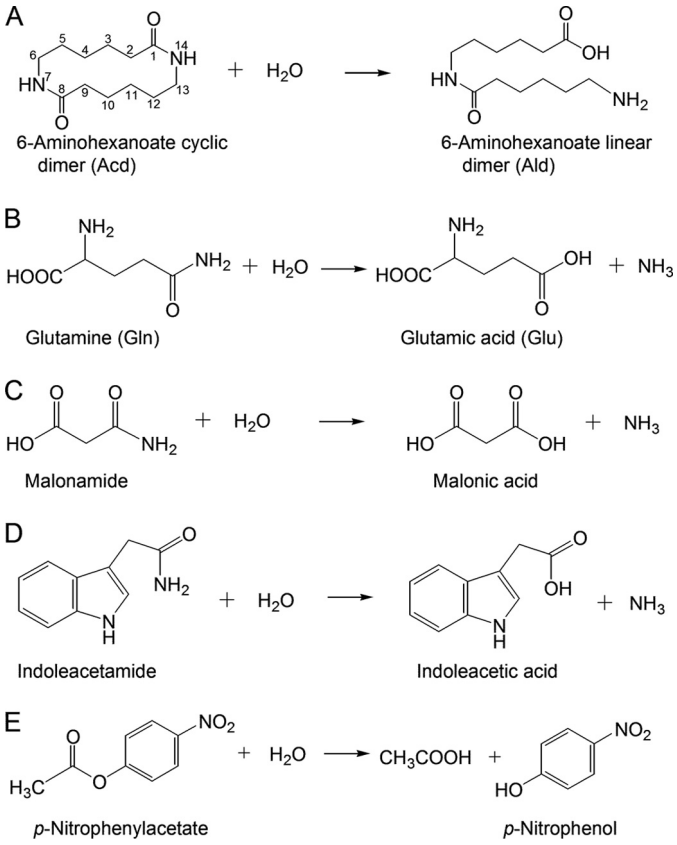

FIGURE 1. **Hydrolysis of various amide and ester compounds.** *A*, Acd. *B*, Gln. *C*, malonamide. *D*, indoleacetamide. *E*, *p*-nitrophenylacetate (C2-ester).

the root mean square deviations of the superimposed C_α atoms were calculated to be 2.2–2.4 Å. The loop region flanked by β9 and H17 in NylA was 10–14 residues longer than the corresponding region in the other AS superfamily enzymes (supplemental Figs. S1 and S2). As discussed below, we suggest that dynamic motion of this flexible loop is important for the catalytic function of NylA.

Functional Comparison with Typical AS Superfamily Enzymes

To examine the activity of NylA on substrates recognized by typical AS superfamily enzymes, we examined glutaminase, malonamidase, and indoleacetamide hydrolase activity in NylA (Fig. 1, *B–D*). TLC analyses demonstrated that the product (Ald) was detected from Acd within 2 h of the reaction using purified NylA (0.1 mg ml^{-1}). In contrast, no detectable amount of product (Glu) was obtained from the substrate (Gln), even after continuing the reaction for 48 h using 1 mg ml^{-1} of NylA (data not shown). This suggests that the glutaminase activity caused by NylA was less than 0.5% of the level of Acd hydrolytic activity. Moreover, the hydrolytic activity of NylA for malonamide and indoleacetamide is ~0.1% of the level of its activity for Acd. These results demonstrate that NylA specifically recognizes Acd as a preferred substrate irrespective of the structural conservations with other AS superfamily enzymes. In contrast, NylA had hydrolytic activity for *p*-nitrophenylacetate (C2-ester), *p*-nitrophenylbutyrate (C4-ester), and *p*-nitrophenyloctanoate (C8-ester), which are almost equivalent to the level of activity for Acd (Fig. 1*E* and Table 2). The structural basis for substrate recognition, on the basis of the enzyme/substrate interaction, is discussed below.

Enzyme/Substrate Interaction

Catalytic Residues—In AS superfamily enzymes, the Ser-*cis*-Ser-Lys triad has been proposed to make up the catalytic residues (8–21). The NylA triad (Ser^{174}-*cis*-Ser^{150}-Lys^{72}) spatially shares a similar position with that of MAE2 (Ser^{155}-*cis*-Ser^{131}-

TABLE 2

Effect of amino acid substitution in NylA on Acd hydrolytic and esterolytic activity

The effects of amino acid substitutions at positions 72, 150, 174, 125, and 316 were tested using purified NylA and its mutant enzymes. Enzyme activities for 10 mM Acd, 0.2 mM *p*-nitrophenylacetate (C2-ester), 0.2 mM *p*-nitrophenylbutyrate (C4-ester), and 0.2 mM *p*-nitrophenyloctanoate (C8-ester) were assayed. The specific activity (μmol min^{-1}(units) mg^{-1}) was estimated for each enzyme. The numbers in parentheses indicate the activity relative to the specific activity of wild-type NylA. Acd hydrolytic activity was assayed in duplicate, and the average value was calculated. The deviations were found to be less than 2%.

	Acd hydrolytic activity	Esterase activity		
		C2-ester	C4-ester	C8-ester
	units mg^{-1}		*units* mg^{-1}	
Wild type	4.17 (100)	1.91 ± 0.02 (100)	1.78 ± 0.06 (100)	1.48 ± 0.08 (100)
K72A	<0.002	<0.001	<0.001	<0.001
S150A	<0.001	<0.001	<0.001	<0.001
S174A	<0.001	<0.001	<0.001	<0.001
N125A	0.57 (13.7)	1.37 ± 0.01 (71.7)	1.11 ± 0.02 (62.3)	1.05 ± 0.02 (70.9)
C316A	0.73 (17.5)	1.73 ± 0.01 (90.6)	1.92 ± 0.03 (108)	1.49 ± 0.04 (101)
C316S	4.46 (107)	3.10 ± 0.14 (162)	2.53 ± 0.14 (142)	3.33 ± 0.23 (225)
C316G	7.70 (185)	2.38 ± 0.06 (125)	2.29 ± 0.08 (129)	1.83 ± 0.07 (124)
C316D	0.063 (1.51)	0.82 ± 0.03 (42.9)	1.48 ± 0.08 (83.1)	1.01 ± 0.01 (68.2)
C316E	0.040 (0.96)	1.13 ± 0.02 (59.2)	1.50 ± 0.09 (84.3)	0.96 ± 0.06 (64.9)
C316N	0.18 (4.32)	0.83 ± 0.01 (43.5)	1.12 ± 0.06 (62.9)	0.75 ± 0.05 (50.7)
C316K	0.15 (3.60)	0.84 ± 0.05 (44.0)	1.11 ± 0.01 (62.4)	0.82 ± 0.02 (55.4)

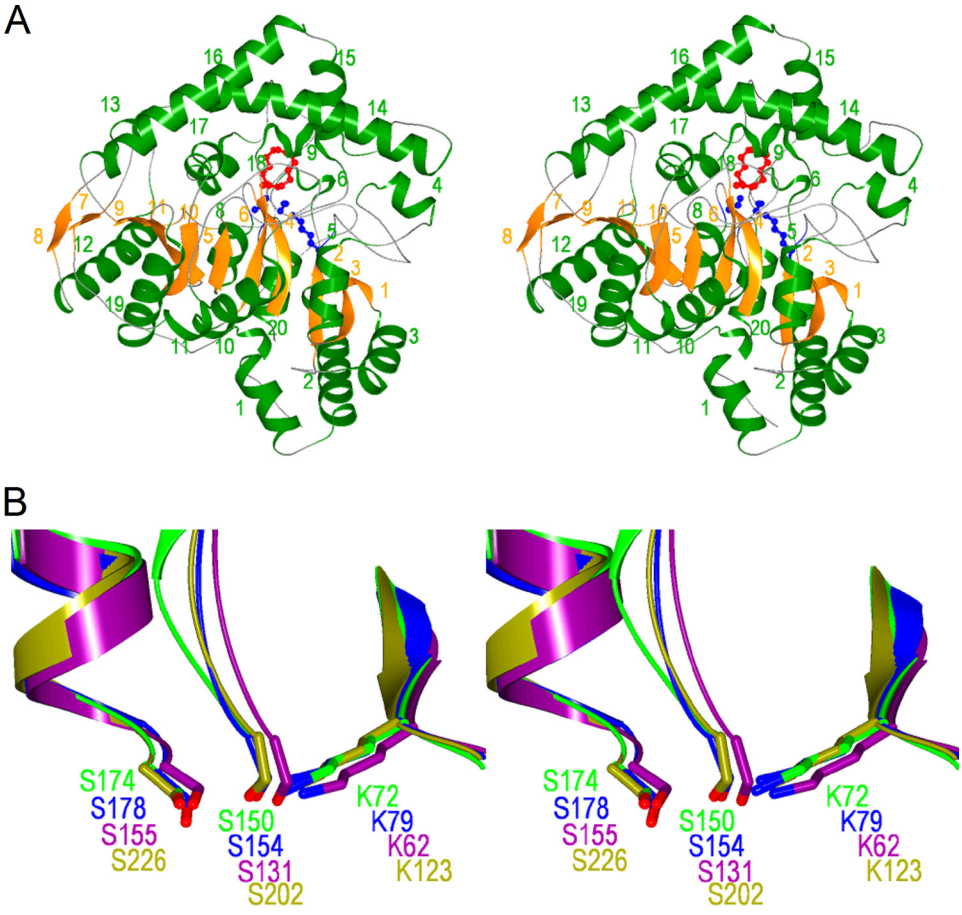

FIGURE 2. **Stereoviews of NylA structures.** *A*, ribbon diagram of the overall structure of NylA. α-Helices and β-strands are colored in *green* and *orange*, respectively, with the number shown in Fig. S1. Substrate Acd and catalytic residues (Lys^{72}, *cis*-Ser^{150}, and Ser^{174}) are shown by a "ball and stick diagram" colored in *red* and *blue*, respectively. *B*, superimposition of NylA structure (*green*) with glutamyl-$tRNA^{Gln}$ amidotransferase subunit A (Protein Data Bank code 2df4; *blue*), malonamidase E2 (Protein Data Bank code 1ocm; *purple*), and peptide amidase (Protein Data Bank code 1m21; *olive*). Superimposition was carried out for the Ser-*cis*-Ser-Lys catalytic triad and its linked region on the transformation matrix generated by secondary structure matching (45).

Lys^{62}), GatA (Ser^{178}-*cis*-Ser^{154}-Lys^{79}), and PAM (Ser^{226}-*cis*-Ser^{202}-Lys^{123}) (Fig. 2*B*). To examine whether the NylA triad is responsible for catalytic function, we individually replaced Ser^{174}, *cis*-Ser^{150}, and Lys^{72} with Ala by site-directed mutagenesis, purified the mutant enzymes to homogeneity, and assayed the enzymatic activities under "standard assay conditions" (10 mM Acd). Single S174A, S150A, or K72A mutations resulted in drastic decreases in Acd hydrolytic and esterolytic activities to undetectable levels (<0.001 unit mg^{-1}) (Table 2), indicating that the Ser^{174}-*cis*-Ser^{150}-Lys^{72} triad is responsible for NylA function.

To analyze the enzyme/substrate interactions, we performed x-ray crystallographic analysis of NylA-A^{174} (S174A mutant of NylA)·Acd complex at 1.80 Å resolution (Table 1). Amino acid residues and Acd substrate in the catalytic cleft gave a clear electron density distribution for which structural models could be determined (Fig. 3). Superimposition of the Acd-bound structure with the unbound structure revealed that the root mean square deviation at C^{α} is smaller than 0.1 Å for the overall structures. Interestingly, Acd is entirely trapped inside the protein molecules upon Acd binding (Figs. 2*A*, 3*B*, and 4). Accessibility of the substrate and water molecules to the catalytic center is discussed below.

In most Ser-reactive hydrolases, the reaction steps of catalysis are divided into acylation and deacylation steps (30, 31). During acylation, the catalytic reactions are initiated by nucleophilic attack of Ser-$O^{\gamma-}$ to the electrophilic carbonyl carbons of amide bonds in the substrate. Therefore, questions are raised as to what residue functions as a nucleophile. X-ray crystallographic analysis of NylA and the NylA-A^{174}·Acd complex suggested that the environment around Ser^{174}-O^{γ} is not sufficiently polar to promote deprotonation of Ser^{174}-$O^{\gamma}H$. In

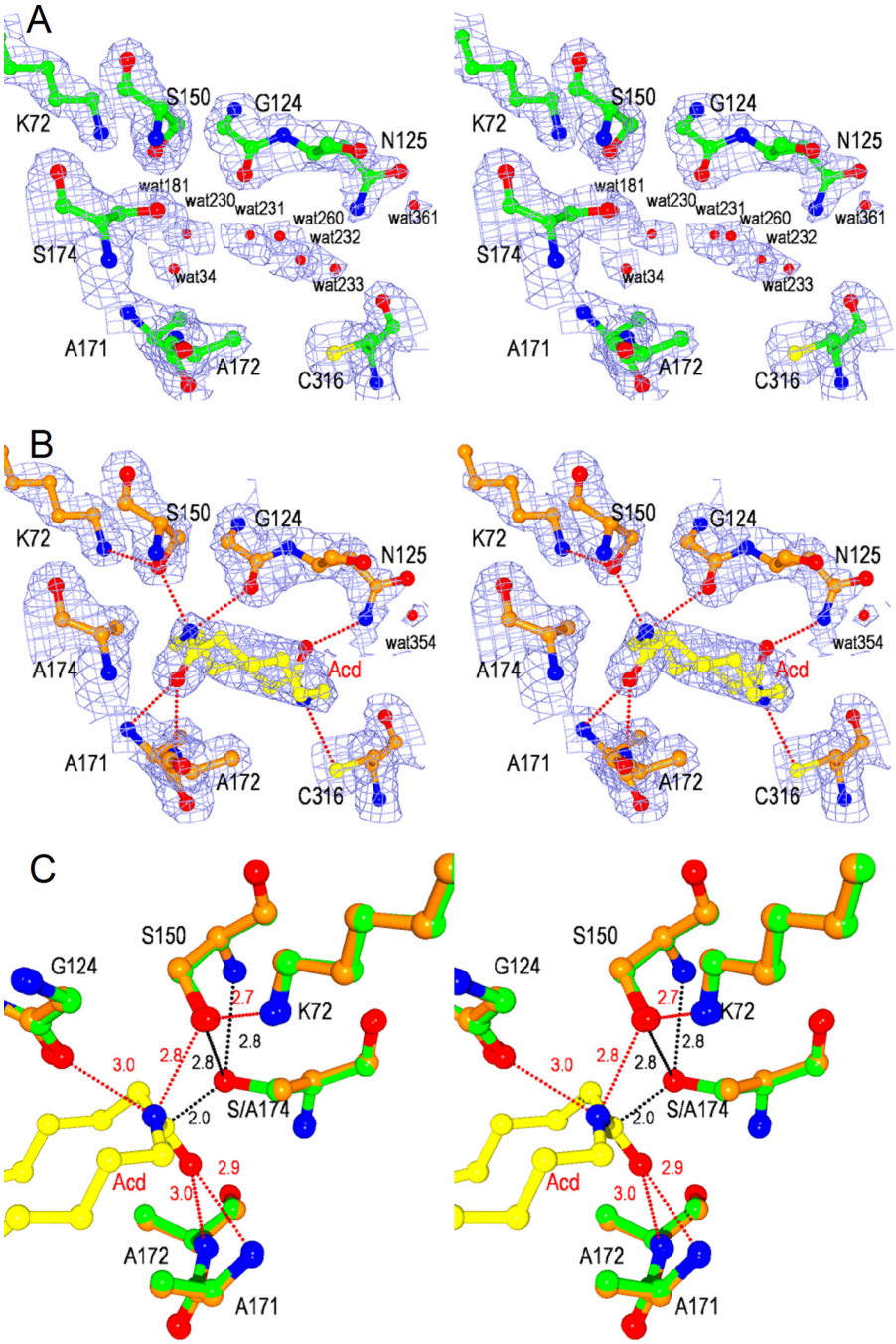

FIGURE 3. **Stereoviews of catalytic cleft of NylA and NylA-A^{174}·Acd complex.** *A* and *B*, 2*Fo* − *Fc* electron density maps of NylA (*green*) (*A*) and the NylA-A^{174}·Acd complex (*orange*) (*B*) contoured at 1.0 σ. Side chain atoms of catalytic/binding residues (Lys^{72}, Gly^{124}, Asn^{125}, *cis*-Ser^{150}, Ala^{171}, Ala^{172}, Ser^{174} (Ala^{174}), and Cys^{316}), water molecules, and substrate Acd are shown. *C*, structure around catalytic residues of NylA (*green*) was superimposed with that around corresponding residues of the NylA-A^{174}·Acd complex (*orange*). Carbon, nitrogen, and oxygen atoms in substrate Acd are shown in *yellow*, *blue*, and *red*, respectively. Possible hydrogen bonds are indicated as *red dotted lines* with the distances in angstroms.

addition, because Ser^{174}-O$^{\gamma}$H is ~4.8 Å away from Lys^{72}-N$^{\zeta}$, it is unlikely that Lys^{72} directly participates in eliminating the proton from Ser^{174}-O$^{\gamma}$H (Fig. 3). However, Ser^{150} exhibited an unusual *cis*-conformation. We estimate that low steric hindrance of Ser^{150} for the backbone structures, because of the presence of consecutive Gly^{148}/Gly^{149} residues, should allow the unusual *cis*-conformation of Ser^{150}. Ser^{174}-O$^{\gamma}$ is spatially 2.8 Å from either *cis*-Ser^{150}-O$^{\gamma}$ or *cis*-Ser^{150}-N (backbone) (Fig. 3*C*). This spatial location should enable Ser^{174}-O$^{\gamma}$ to form hydrogen bonds simultaneously with *cis*-Ser^{150}-O$^{\gamma}$ and *cis*-Ser^{150}-N. Because of the dual hydrogen bonding, it is likely that Ser^{174}-O$^{\gamma}$ favors a deprotonated form even at physiological pH, resulting in the increase in nucleophilicity of Ser^{174} (Fig. 5, *A* and *B*).

It should be noted that the CD spectrum of the Ala^{150} mutant was found to be similar to that of wild-type NylA (supplemental Fig. S3*A*). This result indicates that substitution of Ser^{150}, which has an unusual *cis*-conformer, with Ala does not cause misfolded proteins. Moreover, the Ala^{150} mutant has no detectable activity (<0.001 unit mg^{-1}) under any assay conditions using different Acd concentrations (0.625, 1.25, 2.5, 5.0, and 10.0 mM; almost maximum solubility in water) and an enzyme sample that has been concentrated 20-fold (2.07 mg ml^{-1}). On the basis of these findings, we estimated that turnover (k_{cat}) of the Ala^{150} mutant is <0.001 s^{-1}. Similar roles of *cis*-Ser for increasing the nucleophilicity of catalytic Ser have been proposed for PAM and MAE2 (12, 16).

Substrate-binding Residues—Structural analysis of NylA and the NylA-A^{174}·Acd complex revealed that six hydrogen bonds are possible between NylA and Acd (Fig. 3*B*). Among the four hydrogen bonds connecting to cleaved amide linkages in Acd, two bonds, from Acd-C^{1}-carbonyl O to Ala^{171}-N (backbone) and to Ala^{172}-N (backbone), are estimated to be responsible for oxyanion stabilization (see "Proposed Catalytic Mechanisms"), whereas the other two bonds, from Acd-N^{14} to Gly^{124}-O (backbone) (3.0 Å) and to *cis*-Ser^{150}-O$^{\gamma}$ (2.8 Å), are estimated to be involved in Acd binding (Fig. 3*C*). In addition, at the uncleaved amide linkage in Acd, two hydrogen bonds, from Acd-N^{7} to Cys^{316}-S$^{\gamma}$ (3.2 Å) and from Acd-C^{8}-carbonyl O to Asn^{125}-N$^{\epsilon}$ (2.7 Å), were identified (Fig. 3*B*). In the multiple three-dimensional structural alignments, Cys^{316} in NylA is altered to Ala^{313} (GatA), Gln^{277} (MAE2), or Leu363 (PAM), suggesting that the interaction at position 316 is unique for NylA. Similarly, Asn^{125} in NylA is altered to Met^{129} (GatA) and Ser^{112}

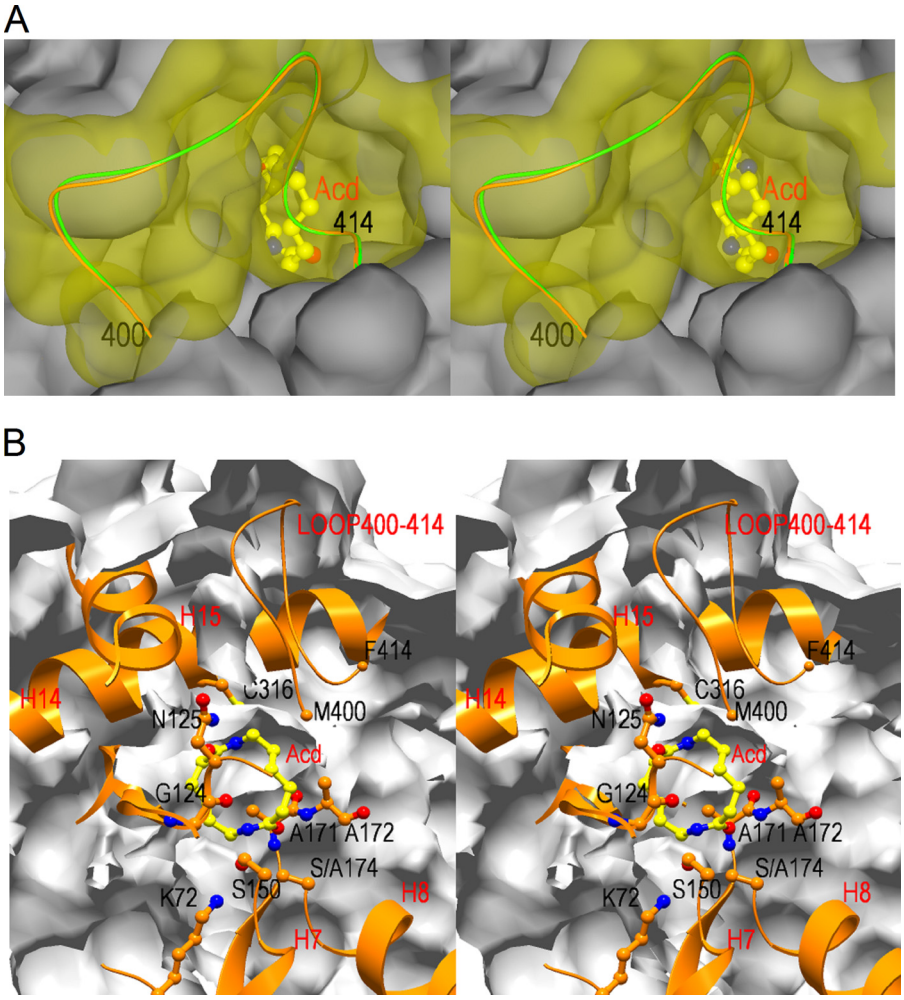

FIGURE 4. **Surface structures of the entrance of the catalytic cleft of NylA-A^{174}·Acd complex.** *A*, stereoview of the entrance of the catalytic cleft. The flexible loop region (positions 400–414) is shown in *yellow*, whereas rest of the region is shown in *gray*. *B*, stereoview of cross-section, including catalytic/binding residues and substrate Acd. The main chain folding (ribbon diagram) and side chain (ball and stick diagram) of catalytic/binding residues (Lys^{72}, Gly^{124}, Asn^{125}, *cis*-Ser^{150}, Ala^{171}, Ala^{172}, Ser^{174} (Ala^{174}), and Cys^{316}) are shown. The surface is shown as a gray layer. Carbon, nitrogen, and oxygen atoms in substrate Acd are shown in *yellow*, *blue*, and *red*, respectively.

(MAE2), although Asn^{125} is conserved as Asn^{172} in PAM (supplemental Fig. S1).

To examine the effect of amino acid substitutions at positions 125 and 316 on catalytic function, we constructed the N125A and C316A mutants by site-directed mutagenesis. Assays under standard conditions showed that hydrolytic activity was ~14% (Ala^{125} mutant) and 18% (Ala^{316} mutant) of the wild-type NylA level (Table 2). A kinetic study showed that the N125A mutation increased the K_m ~4-fold, suggesting that the decrease in substrate-binding is due to the loss of hydrogen bonding between the Acd-C^{8}-carbonyl O and the Asn^{125}-N$^{\epsilon}$. Similarly, the C316A substitution should result in the loss of hydrogen bonding between Acd-N^{7} and Cys^{316}-S$^{\gamma}$. However, the C316A substitution decreased the K_m to approximately one-quarter the level of wild-type NylA (Table 3). Moreover, these two mutations also decreased the k_{cat} values to 23% (Ala^{125} enzyme) and 14% (Ala^{316} enzyme) of the wild-type NylA level.

The effects of amino acid substitutions at position 316 were more extensively examined. It should be noted that the overall protein structures were not affected much by substitutions at the substrate-binding sites, because the CD spectra of the three mutants (N125A, C316S, and C316D) were very similar to the spectrum of wild-type enzyme (supplemental Fig. S3*B*). Substitution to acidic (Glu and Asp), basic (Lys), or other polar (Asn) residues decreased the activity to 1–4% of the wild-type level (Table 3). Although the C316S substitution had no significant effect on activity under standard assay conditions, a kinetic study showed that the K_m for Acd had decreased from 3.5 mM (wild-type NylA) to 1.8 mM (Ser^{316} mutant) without affecting the k_{cat}. It is likely that possible hydrogen bonding between the Acd-N^{7} and Ser^{316}-O$^{\gamma}$ more stably positions the substrate than hydrogen bonding with Cys^{316}-S$^{\gamma}$. Unexpectedly, k_{cat} was enhanced in the Gly^{316} mutant without affecting the K_m, even though the C316G mutation should have resulted in the loss of hydrogen bonding at position 316. In contrast, the C316D mutation significantly decreased activity. Because of the limited solubility of Acd in water, it is possible to perform kinetic studies only at concentrations lower than 10 mM Acd. Although the standard error for the calculated K_m value is quite large because of extrapolation to higher concentrations, we found that the calculated K_m value of the Asp^{316} mutant was ~20 mM, which exceeds the saturated Acd concentration, and the k_{cat} value was ~3% the level of wild-type NylA (Table 3). Thus, the binding affinity and turnover of catalysis are estimated to be drastically decreased by C316D substitutions.

However, it should be demonstrated that amino acid substitutions at position 316 had less effect on carboxylesterase activity than Acd hydrolytic activity. Namely, the Acd hydrolytic activity varied 200-fold (0.96–185% the activity of wild-type NylA) among the mutants, whereas the activity for C2-, C4-, and C8-esters was only within the range of 43–225% (Table 2). Substrate recognition between amides and carboxylesters is discussed below with other Ser-reactive hydrolases.

Proposed Catalytic Mechanisms

From the spatial location of catalytic/binding residues and functional analysis by site-directed mutagenesis, we estimated the catalytic mechanisms of NylA (Fig. 5).

Nucleophilic Attack of Ser^{174} and Oxyanion Stabilization—Nucleophilic Ser^{174}-O$^{\gamma-}$ activated by *cis*-Ser^{150} should attack

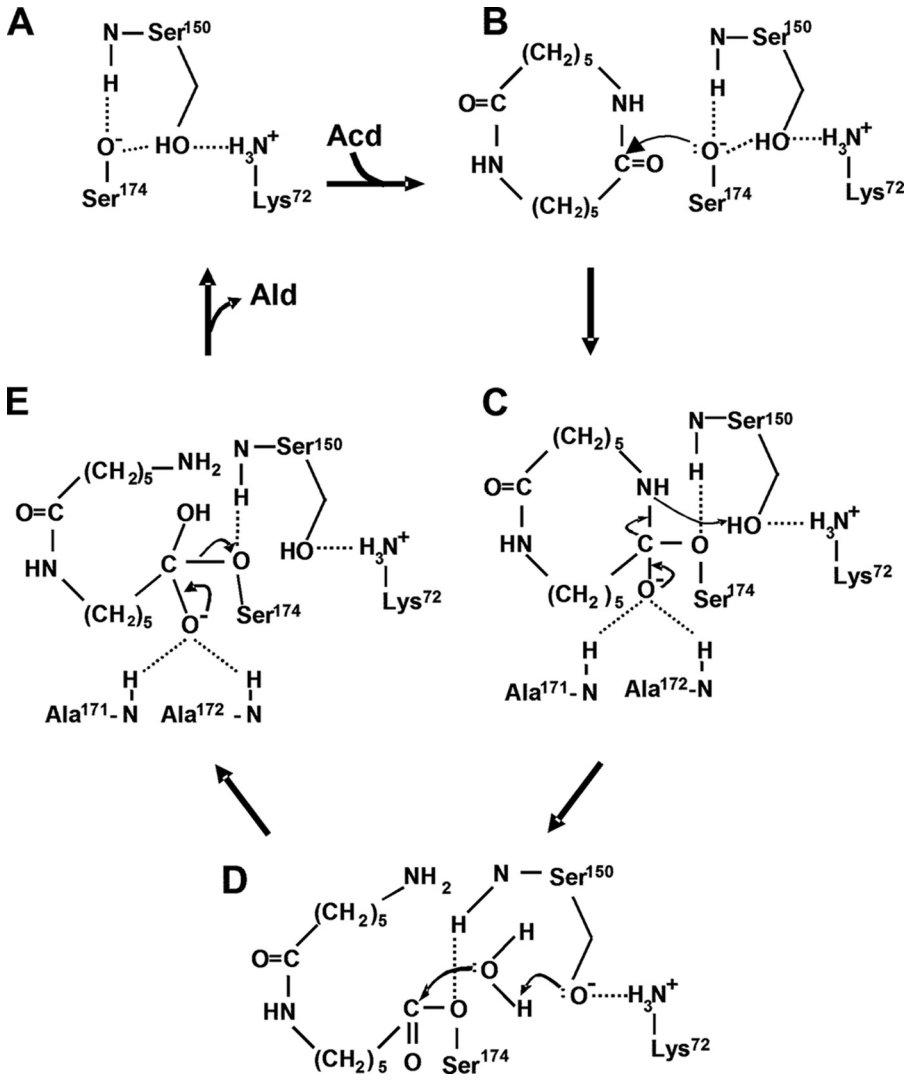

FIGURE 5. **Proposed catalytic mechanism of NylA.** The steps in the catalytic reaction are shown. *A*, free enzyme. *B*, enzyme + substrate. *C*, tetrahedral intermediate. *D*, acyl-enzyme. *E*, tetrahedral intermediate.

TABLE 3

Kinetic parameters of NylA mutant enzymes

Acd hydrolytic activity was assayed using the purified enzymes under standard assay conditions, except that various concentrations of Acd were used.

Mutation	Kinetic study		
	K_m	k_{cat}	k_{cat}/K_m
	mM	s^{-1}	s^{-1} mM^{-1}
Wild type	3.51 ± 0.16	4.97 ± 0.10	1.42
N125A	13.2 ± 0.75	1.12 ± 0.04	0.085
C316A	0.85 ± 0.04	0.71 ± 0.01	0.83
C316S	1.80 ± 0.20	4.83 ± 0.17	2.68
C316G	3.66 ± 0.27	9.15 ± 0.28	2.50
C316D	19 ± 10	0.14 ± 0.05	0.007

the electrophilic carbonyl carbon of the substrate (Fig. 5*B*), with the subsequent formation of a tetrahedral intermediate containing an unstable oxyanion (Fig. 5*C*). Therefore, stabilization of the oxyanion is important for catalytic function. The carbonyl oxygen in Acd is spatially 2.9 and 3.0 Å from the main chain nitrogens of Ala^{171} and Ala^{172}, respectively (Fig. 3*C*). Therefore, we estimate that the oxyanion formed during Acd hydrolytic reaction is stabilized by the positively charged nitrogens at Ala^{171} and Ala^{172} (Fig. 5*C*).

Formation of Acyl-enzyme—To break down the tetrahedral intermediate to the acyl-enzyme, the tetrahedral intermediate should accept a proton from a general acid. Because *cis*-Ser^{150}-O$^{\gamma}$ is close to Acd-N^{14} (nitrogen of cleaved amide linkage in Acd) (distance, 2.8 Å) (Fig. 3*C*), it should be possible that *cis*-Ser^{150}-O$^{\gamma}$H functions as the general acid, providing a proton to the departing amino group (Fig. 5*C*). The proton transfer should be facilitated by the amino group of Lys^{72}-NH$_3^+$, which can stabilize the deprotonated Ser^{150}-O$^{\gamma-}$ (2.7 Å from Lys^{72}-NH$_3^+$) (Figs. 3*C* and 5*C*). Thus, *cis*-Ser^{150} and Lys^{72} should be involved in facilitating proton transfer and maintaining the optimum electrostatic environment to promote the acylation of Ser^{174}.

Deacylation—Conversion of the acyl-enzyme to free enzyme (deacylation) generally requires two steps, *i.e.* formation of a tetrahedral intermediate through nucleophilic attack of a water molecule (Fig. 5*D*) and regeneration of free enzyme (Fig. 5*E*). In NylA, water molecules responsible for deacylation have not been found around the catalytic center in the Acd-bound structure (Fig. 3*B*). However, as discussed below, we estimate that the enzyme accepts water molecules for deacylation from solvent water through the dynamic motion of a flexible loop region (Phe^{400}–Phe^{414}) (Fig. 4 and supplemental Fig. S4). The incorporated water molecule should function as a nucleophile to form a tetrahedral intermediate, and the resulting tetrahedral intermediate should be stabilized by Ala^{171}-N$^+$ and Ala^{172}-N$^+$ (Fig. 5*E*), in a similar fashion as the acylation step. Finally, the intermediate should be hydrolyzed to Ald plus free enzyme, which reinitiates the successive catalytic cycle.

Accessibility of Substrate to Catalytic Center

The catalytic (Ser^{174}, *cis*-Ser^{150}, Lys^{72}) and binding (Asn^{125} and Cys^{316}) residues in NylA are located at β2 (Lys^{72}), H7 (*cis*-Ser^{150}), H8 (Ser^{174}), H6 (Asn^{125}), and H14 (Cys^{316}) (supplemental Fig. S1). Through these interactions, NylA should hold Acd inside the catalytic cleft, surrounded by stable secondary structures (Fig. 4*B*). Therefore, questions are raised regarding how the Acd substrate can penetrate close to the catalytic residues located near the center of the globular protein molecule. As stated above, the loop region (Thr^{388}–Phe^{414}), flanked by β9 and H17 in NylA, is 10–14 residues longer than the corresponding regions in MAE2, PAM, and GatA (supplemental Fig.

S1). It is likely that the longer loop makes it more flexible. Actually, crystallographic analysis of NylA revealed that the atomic B-factors of amino acid residues are significantly large (80–95 Å^2), especially at Phe^{400}–Arg^{410}, compared with helices, β-strands, and the other loop regions (supplemental Fig. S4). Because the atomic B-factors correlate with the degree of thermal motion and spatial disorder in the crystal structures, the structure of the loop should significantly deviate during the enzymatic reaction. Interestingly, the flexible loop (Phe^{410}–Phe^{414}) region forms a catalytic cleft with a long helix (H14) and short helix (H15), including catalytic/binding residues (Fig. 4). We suggest that the dynamic motion of the loop located between β-strand 9 (β9) and Helix 17 (H17) allows Acd to incorporate into the cleft, including the catalytic center. Assuming that the substrate is incorporated in this manner, the catalytic triads (Ser^{174}-*cis*-Ser^{150}-Lys^{72}) are located at the bottom of the catalytic cleft, whereas the binding residues (Asn^{125} and Cys^{316}) are localized closer to the entrance of the cleft.

Water Molecules

In most hydrolases, the catalytic sites are open to solvent, so the enzyme can accept water molecules for deacylation from the massive solvent environment. In class A β-lactamase, hydrolytic water, activated by Glu^{166}, is considered to be responsible for either the acylation or deacylation step (32–34). In NylA, 521 and 445 water molecules were identified for Acd-bound and unbound structures, respectively. Larger numbers of water molecules in substrate-bound structures are thought to be due to the higher resolutions. In unbound structures, seven water molecules (Wat34, Wat181, Wat230, Wat231, Wat232, Wat233, and Wat260) were identified in the cleft around the catalytic residues (Fig. 3*A*). However, in the enzyme·substrate complex, these water molecules are replaced with Acd, and no water molecules generating hydrogen bonds with substrate or catalytic residues can be identified (Fig. 3*B*). Wat354 in the NylA-A^{174}·Acd complex (Wat361 in the unbound enzyme) is 3.5 Å from Asn^{125}-N$^{\epsilon}$. However, Wat354 is close to uncleaved amide linkages in Acd and therefore is not considered to be responsible for deacylation. These results suggest that the enzyme accepts water molecules responsible for deacylation during the dynamic motion of the flexible loop regions.

Even after completing the stage of acylation, no reaction product should be released from NylA utilizing cyclic amide compounds as substrate (Fig. 5*D*), whereas first reaction product is released from ordinary protease/esterase utilizing the linear amide/ester compounds. Therefore, the bulky *N*-(6-aminohexanoyl)-6-aminohexanoyl group in the acyl-NylA enzyme transiently alters the position of the flexible loop, which allows the penetration of water molecules to the catalytic center. Alternatively, the loop region flexibly fluctuates regardless of the presence or absence of substrate and freely accepts water molecules from the solvent environment. In either case, dynamic motion of the flexible loop associated with the uptake of substrate/water molecules and release of product should be essential for the catalytic reaction of NylA.

Comparison with Other Ser-reactive Hydrolases and Evolutionary Implications

Typical Ser-proteases (trypsin, *etc.*) and lipase/esterases possess a classical Ser-His-Asp(Glu) triad, in which His abstracts the proton of Ser-OH and Asp (Glu) promotes the role of His by stabilizing the positively charged His-imidazole (30, 31). Another catalytic triad, Ser-Tyr-Lys, has been identified in NylB (Ald-hydrolase) (37–41), NylB′ carboxylesterase (37–41), EstB carboxylesterase (42), DD-peptidase (43), and class C β-lactamase (44). NylB and a NylB/NylB′ hybrid protein (Hyb24DN; having a NylB-level of Ald hydrolytic activity) effectively recognize substrates having 6-aminohexanoate (nylon unit) as N-terminal residues in the substrate but possess activities for various carboxylesters (37–41).

X-ray crystallographic analysis of Hyb-24DN (a NylB/NylB′ hybrid) and its Ald-bound structure demonstrates that Ald binding induced the transition from the open (substrate-unbound) form to the closed (substrate-bound) form through the dynamic motion of the loop region and the flip-flop of Tyr^{170}, whereas the enzyme performs the catalytic function as a relaxed open form during the entire catalytic cycle as a carboxylesterase (38). This model is consistent with our finding that Ald hydrolytic activity is significantly affected by amino acid substitutions at positions 170, 181, 187, 264, 266, and 370, responsible for Ald binding, whereas amino acid substitutions at these positions barely affect the esterase activity (37–41). A molecular dynamic simulation for NylB/NylB′ has suggested that the substrate-unbound open form is maintained at an energy minimum and requires activation energy to transition to the substrate-bound closed form (38). In addition, water molecules incorporated into the catalytic cleft are excluded in the closed form but regained from the solvent water at deacylation with a back transition to the open form. We have speculated that the release of 6-aminohexanoate (corresponding to the C-terminal half of Ald) triggers the penetration of water molecules to the catalytic center (38). On the basis of these results, we have proposed that NylB has evolved from a pre-existing esterase with a β-lactamase fold (37–41).

Present x-ray crystallographic analysis revealed that NylA is classified as a member of the AS superfamily and utilizes the distinct catalytic triad Ser-*cis*-Ser-Lys. Although NylA possesses broad specificity for carboxylesters, we estimate that the unique substrate specificity of NylA recognizing the nylon-6 byproduct should be achieved by incorporating amino acid residues responsible for Acd-binding while utilizing the common Ser-*cis*-Ser-Lys catalytic triad conserved in the AS superfamily. Thus, the new enzyme acting on the nylon-6 byproduct seems to diverge from ancestral proteins to create families composed of highly specialized enzymes.

In malonamidase E2 (MAE2, an AS family enzyme), the catalytic activity is drastically decreased by R158E and R158Q mutations, and the k_{cat} value of the R158K mutant is similar to that of wild type with a K_m value increased by 100-fold (13). In Hyb-24DN, Asp^{181}-COO^- is responsible for electrostatic stabilization of Ald-NH_3^+, and D181K and D181H substitutions decreased the activity by >10,000-fold (37, 38). In contrast to the drastic effect by electrostatic stabilization, D370Y substitu-

tion in NylB′-type carboxylesterase (Hyb-24) increased the Ald hydrolytic activity by 8.2-fold, concomitant with formation of a hydrogen bond with substrate Ald. Thus, we roughly estimate that the energetic contribution of a hydrogen bond contributes a ~10-fold difference in binding affinity (39–41). However, the "improvements" in NylA activity caused by substitution at position 316 are extremely modest. We suggest that that the effects of amino acid substitution at the Acd-binding sites in NylA are summarized as follows: (i) Even if the hydrogen bond at Acd-N^7 is eliminated, close contact with the substrate and inner surface of the protein molecule still stably holds the substrate inside the globular protein. (ii) Because of the inflexible compact structure of Acd trapped in the catalytic cleft, amino acid substitutions interacting at the uncleaved site (Acd-N^7) affect the suitable positioning of the cleaved site (Acd-C^1/Acd-N^{14}) against the catalytic residues, resulting in the decrease in k_{cat}. (iii) Substitution of Cys^{316} to a bulky/polar residue (Glu, Asp, Asn, and Lys), located at the entrance of the catalytic cleft, has a negative effect on the incorporation of the substrate into the catalytic cleft, resulting in a decrease in enzyme activity. In particular, replacement to acidic residues (Glu and Asp) significantly decreases the activity, probably because of an electrostatic effect. Finally, it should be noted that plasmid-encoded NylA from *Arthrobacter* and *Pseudomonas* and ω-laurolactam hydrolase from *Rhodococcus*, *Cupriavidus*, and *Sphingomonas* exhibit 98–99% overall homology, although these strains have been isolated independently and classified as different genera. These results may imply that the *nylA*-related genes have been recently distributed among microorganisms in the course of evolution, probably by plasmid-mediated gene transfer (4–7, 35, 36).

Acknowledgment—We thank Prof. Yuji Goto (Osaka University) for analyzing the CD spectra of NylA and its mutant enzymes.

REFERENCES

1. Negoro, S. (2000) *Appl. Microbiol. Biotechnol.* **54,** 461–466
2. Negoro, S. (2002) *Biopolymers* **9,** 395–415
3. Kinoshita, S., Negoro, S., Muramatsu, M., Bisaria, V. S., Sawada, S., and Okada, H. (1977) *Eur. J. Biochem.* **80,** 489–495
4. Kanagawa, K., Negoro, S., Takada, N., and Okada, H. (1989) *J. Bacteriol.* **171,** 3181–3186
5. Tsuchiya, K., Fukuyama, S., Kanzaki, N., Kanagawa, K., Negoro, S., and Okada, H. (1989) *J. Bacteriol.* **171,** 3187–3191
6. Yasuhira, K., Tanaka, Y., Shibata, H., Kawashima, Y., Ohara, A., Kato, D., Takeo, M., and Negoro, S. (2007) *Appl. Environ. Microbiol.* **73,** 7099–7102
7. Kato, K., Ohtsuki, K., Koda, Y., Maekawa, T., Yomo, T., Negoro, S., and Urabe, I. (1995) *Microbiology* **141,** 2585–2590
8. Schmitt, E., Panvert, M., Blanquet, S., and Mechulam, Y. (2005) *Structure* **13,** 1421–1433
9. Nakamura, A., Yao, M., Chimnaronk, S., Sakai, N., and Tanaka, I. (2006) *Science* **312,** 1954–1958
10. Neu, D., Lehmann, T., Elleuche, S., and Pollmann, S. (2007) *FEBS J.* **274,** 3440–3451
11. Yamada, T., Palm, C. J., Brooks, B., and Kosuge, T. (1985) *Proc. Natl. Acad. Sci. U.S.A.* **82,** 6522–6526
12. Shin, S., Lee, T. H., Ha, N. C., Koo, H. M., Kim, S. Y., Lee, H. S., Kim, Y. S., and Oh, B. H. (2002) *EMBO J.* **21,** 2509–2516
13. Yun, Y. S., Lee, W., Shin, S., Oh, B. H., and Choi, K. Y. (2006) *J. Biol. Chem.* **281,** 40057–40064
14. Bracey, M. H., Hanson, M. A., Masuda, K. R., Stevens, R. C., and Cravatt, B. F. (2002) *Science* **298,** 1793–1796
15. Wei, B. Q., Mikkelsen, T. S., McKinney, M. K., Lander, E. S., and Cravatt, B. F. (2006) *J. Biol. Chem.* **281,** 36569–36578
16. Labahn, J., Neumann, S., Büldt, G., Kula, M. R., and Granzin, J. (2002) *J. Mol. Biol.* **322,** 1053–1064
17. Valiña, A. L., Mazumder-Shivakumar, D., and Bruice, T. C. (2004) *Biochemistry* **43,** 15657–15672
18. Kobayashi, M., Goda, M., and Shimizu, S. (1998) *FEBS Lett.* **439,** 325–328
19. Cilia, E., Fabbri, A., Uriani, M., Scialdone, G. G., and Ammendola, S. (2005) *FEBS J.* **272,** 4716–4724
20. Asano, Y., Fukuta, Y., Yoshida, Y., and Komeda, H. (2008) *Biosci. Biotechnol. Biochem.* **72,** 2141–2150
21. Heumann, S., Eberl, A., Fischer-Colbrie, G., Pobeheim, H., Kaufmann, F., Ribitsch, D., Cavaco-Paulo, A., and Guebitz, G. M. (2009) *Biotechnol. Bioeng.* **102,** 1003–1011
22. Yasuhira, K., Uedo, Y., Shibata, N., Negoro, S., Takeo, M., and Higuchi, Y. (2006) *Acta Crystallogr. Sect. F Struct. Biol. Cryst. Commun.* **62,** 1209–1211
23. Ito, W., Ishiguro, H., and Kurosawa, Y. (1991) *Gene* **102,** 67–70
24. Otwinowski, Z., and Minor, W. (1997) *Methods Enzymol.* **276,** 307–326
25. Weeks, C. M., Blessing, R. H., Miller, R., Mungee, R., Potter, S. A., Rappleye, J., Smith, G. D., Xu, H., and Furey, W. (2002) *Z. Kristallogr.* **217,** 686–693
26. de La Fortelle, E., and Bricogne, G. (1997) *Methods Enzymol.* **276,** 472–494
27. McRee, D. E. (1993) *Practical Protein Crystallography*, Academic Press, San Diego, CA
28. Brünger, A. T., Adams, P. D., Clore, G. M., DeLano, W. L., Gros, P., Grosse-Kunstleve, R. W., Jiang, J. S., Kuszewski, J., Nilges, N., Pannu, N. S., Read, R. J., Rice, L. M., Simonson, T., and Warren, G. L. (1998) *Acta Crystallogr. D Biol. Crystallogr.* **54,** 905–921
29. Davis, I. W., Leaver-Fay, A., Chen, V. B., Block, J. N., Kapral, G. J., Wang, X., Murray, L. W., Arendall, W. B., 3rd, Snoeyink, J., Richardson, J. S., and Richardson, D. C. (2007) *Nucleic Acids Res.* **35,** W375–W383
30. Fersht, A. R. (1984) *Enzyme Structure and Mechanism* (2nd Ed), pp. 389–452, W. H. Freeman and Co., New York
31. Arpigny, J. L., and Jaeger, K. E. (1999) *Biochem. J.* **343,** 177–183
32. Zawadzke, L. E., Chen, C. C., Banerjee, S., Li, Z., Wäsch, S., Kapadia, G., Moult, J., and Herzberg, O. (1996) *Biochemistry* **35,** 16475–16482
33. Minasov, G., Wang, X., and Shoichet, B. K. (2002) *J. Am. Chem. Soc.* **124,** 5333–5340
34. Hermann, J. C., Ridder, L., Mulholland, A. J., and Höltje, H. D. (2003) *J. Am. Chem. Soc.* **125,** 9590–9591
35. Okada, H., Negoro, S., Kimura, H., and Nakamura, S. (1983) *Nature* **306,** 203–206
36. Yasuhira, K., Uedo, Y., Takeo, M., Kato, D., and Negoro, S. (2007) *J. Biosci. Bioeng.* **104,** 521–524
37. Negoro, S., Ohki, T., Shibata, N., Mizuno, N., Wakitani, Y., Tsurukame, J., Matsumoto, K., Kawamoto, I., Takeo, M., and Higuchi, Y. (2005) *J. Biol. Chem.* **280,** 39644–39652
38. Negoro, S., Ohki, T., Shibata, N., Sasa, K., Hayashi, H., Nakano, H., Yasuhira, K., Kato, D., Takeo, M., and Higuchi, Y. (2007) *J. Mol. Biol.* **370,** 142–156
39. Ohki, T., Wakitani, Y., Takeo, M., Yasuhira, K., Shibata, N., Higuchi, Y., and Negoro, S. (2006) *FEBS Lett.* **580,** 5054–5058
40. Kawashima, Y., Ohki, T., Shibata, N., Higuchi, Y., Wakitani, Y., Matsuura, Y., Nakata, Y., Takeo, M., Kato, D., and Negoro, S. (2009) *FEBS J.* **276,** 2547–2556
41. Ohki, T., Shibata, N., Higuchi, Y., Kawashima, Y., Takeo, M., Kato, D., and Negoro, S. (2009) *Protein Sci.* **18,** 1662–1673
42. Wagner, U. G., Petersen, E. I., Schwab, H., and Kratky, C. (2002) *Protein Sci.* **11,** 467–478
43. Silvaggi, N. R., Anderson, J. W., Brinsmade, S. R., Pratt, R. F., and Kelly, J. A. (2003) *Biochemistry* **42,** 1199–1208
44. Nukaga, M., Kumar, S., Nukaga, K., Pratt, R. F., and Knox, J. R. (2004) *J. Biol. Chem.* **279,** 9344–9352
45. Laskowski, R. A., McArthur, M. W., Moss, D. S., and Thornton, J. M. (1993) *J. Appl. Crystallogr.* **265,** 283–291